Understanding very faint X-ray binaries from X-ray light curves

Simon van Eeden
Supervised by Nathalie Degenaar

Anton Pannekoek Institute, University of Amsterdam
July 14, 2021
Draft version

ABSTRACT

Very Faint X-ray binaries having peak luminosity's of 10^{34-36} erg s^{-1} are still not fully understood. We have performed a first systematic analysis of outburst light curves from 21 sources by determining the duration and decay time. The distribution of the duration and decay time of each outburst appears very similar to bright X-ray binaries hinting to a similar accretion process. We have used the disc instability model to probe the disc radius and orbital period. For 7 sources this resulted in orbital periods of two to five hours as expected indicating that the accretion process behind Very Faint X-ray binaries is similar to bright X-ray binaries.

VU VRIJE UNIVERSITEIT AMSTERDAM | UNIVERSITEIT VAN AMSTERDAM

Populaire samenvatting

Röntgendubbelster systemen bestaan uit een neutronen ster of een zwart gat en een donor ster die om elkaar heen draaien. Doordat neutronon sterren en zwarte gaten zo zwaar zijn kunnen ze materie van de buitenste lagen van de donor ster naar zich toe trekken. Hierdoor ontstaat er een stroom van materie richting het compacte object wat we ook wel accretie noemen. Deze stroom orienteerd zich dusdanig dat er een schijf met materie ontstaat rondom het compacte object. Door instabiliteit in deze schijf kunnen er uitbarstingen ontstaan waarbij in een aantal dagen tot weken erg veel materie op het compacte object valt. Tijdens een uitbarsting ontstaat er tot 10000 keer meer Röntgenstraling wat we met Röntgen telescopen in de ruimte zoals Swift en RXTE kunnen waarnemen.

In dit onderzoek is gekeken naar 21 Röntgendubbelster systemen die erg zwak zijn. Om beter te begrijpen waarom deze systemen zo zwak zijn hebben we van deze systemen de licht curves van uitbarstingen gekarakteriseert. Als eerst hebben we gekeken of deze bronnen een andere lengte en afvaltijd hebben in vergelijking met heldere bronnen. We hebben gevonden dat distributie van de lengte en de afvaltijd van de uitbarstingen van hele zwakke systemen dezelfde trend volgt als die van heldere systemen. We denken dat dit een indicatie geeft dat hele zwakke systemen hetzelfde accretie process volgen als heldere systemen.

Ten tweede hebben we gebruik gemaakt van een stabiliteits model om de omlooptijd van het systeem te kunnen bepalen omdat we verwachten dat deze korter is voor zwakkere systemen. Het stabiliteits model lijkt voor zes systemen de uitbarsting vorm goed te benaderen en geeft voor twee systemen resultaten die overeenkomen met observaties. Alle zes systemen hebben zoals verwacht een korte omlooptijd van 2 tot 6 uur. Dit geeft ons ook een indicatie voor een vergelijkbaar accretieproces in hele zwakke en heldere systemen. Echter geldt voor veel hele zwakke bronnen dat de vorm van de uitbarsting niet altijd duidelijk te zien omdat ze zo zwak zijn. Daarbij hebben we alleen voor 2 bronnen kunnen controleren of het model klopt dus kunnnen we niet met zekerheid zeggen dat het stabiliteitsmodel werkt voor zwakke bronnen. Hiervoor is het nodig om toekomstige uitbarstingen te analyseren met het model.

1 Introduction

A special case of binary systems are X-ray binaries. These systems contain a donor star orbiting a neuron star (NS) or a black hole (BH). The high gravitational forces from these compact objects can cause accretion of matter from the donor star on to the compact object. During accretion X-rays are emitted and can be observed with X-ray telescopes. Observations have shown persistent sources that have a constant accretion rate and emit constant X-rays. But they also show transient sources that are most of the time in quiescence and occasionally show a rise in X-ray. These occasional events are called outbursts and typically last for a couple of days to several weeks while reaching peak luminosity's up to 10^{39} erg s^{-1}. Currently roughly 200 X-ray binaries have been observed (Liu et al. 2007). Since the last 15 years evidence have grown for the existence of Very Faint X-ray Binaries (VFXB) that have outburst peak luminosity's of 10^{34-36} erg s^{-1}. For a long time observations on this subclass were difficult because their brightness approach the instrumental limits. Besides the observational difficulties currently about 30 X-ray binaries are classified as a VFXB.

It is yet not understood why VFXB's are so faint. So far research have been focusing only on individual sources but to find out more about the origin of the faint character a systematic analysis on outburst light curves from multiple VFXB's is required. There have been already systematic studies of outbursts from bright X-ray binaries (Yan and Yu 2015; Chen et al. 1997). Comparing outburst characteristics such as the duration and decay time of very faint X-ray binaries with those of bright sources can provide us more insight in the accretion process of these systems. Secondly it is interesting to test the disc instability model, the generally accepted description for bright outbursts, on very faint x-ray binaries too. So far this model has successfully described the decay shape of several outbursts from bright sources (Powell et al. 2007). Current observations from X-ray binaries predicts lower orbital periods for lower luminosity's (Wu et al. 2010). Still it is unkown if multiple VFXB's match with this hypothesis and the disc instability allows us to test this hypothesis.

To fulfill these needs in exploring the nature of very faint x-ray binaries, we aim to answer the following two questions. What is the typical duration and decay time of outbursts of VFXB's? Do VFXB's have shorter orbital periods?

2 X-ray binary classification

This section contains the required background knowledge in the classification of X-ray binaries. The classification of X-ray binaries involves three criteria: the type of the compact object, the mass of the companion star and the X-ray peak luminosity. The following sections will explain each criteria.

2.1 Type of the compact object

BH

The first classification criteria is the type of compact object; BH or NS. BH's can be identified by calculating their mass. When this mass exceeds the maximum mass of a NS $\sim 2.5 - 3M_{\odot}$ we know the compact object should be a BH. Calculating the mass of the compact object can be a hard task. For this calculation the X-ray binary must be bright enough in quiescence in order to identify the spectra of the donor star. If the orbital plane is aligned with our line of sight the spectral lines are blue shifted when the donor star moves towards us and red shifted when the donor star moves away from us. Knowing the orbital period and the mass of the donor star allows us to derive the mass of the compact object. This method resulted in the identification of *XTE J1118+480* as a BH (Torres et al.

2004).

NS
NS's can be recognized by thermonuclear bursts. These burst happen only on a solid surface and are therefore linked to NS's. They can be detected by spectral analysis (Cornelisse et al. 2002). Another characteristic proving a NS origin is the detection of millisecond pulsations (Ng et al. 2021).

2.2 Mass of companion star

High mass X-ray binaries
High mass transients can accrete material by a stellar wind or decretion disk of the companion star. Be/X-ray transients are the most common type for accretion via a decretion disk. Be stars are B or O type stars that can spin so fast that the rotation force overcomes the gravitational force and a decretion disk forms (Wijnands et al. 2006).

Low mass X-ray binaries
In low mass transients mass transfer happens via Roche Lobe overflow during which a accretion disk forms around the compact object. The disc instability model provides a generally accepted description of this accretion processes for bright sources (Lasota 2001). A more detailed description of this model can be found in section 3.

2.3 Luminosity

Bright to very bright
The third classification of X-ray transients is based on their X-ray peak luminosity when they are in outburst. Bright to very bright X-ray binaries have peak luminosity's of 10^{37-38} erg s^{-1} in X-ray. Currently the best description of the accretion behaviour of this class is given by the disc instability model explained in section 3.

Faint
Faint X-ray binaries have peak luminosities of 10^{36-37} erg s^{-1} in X-ray. The faint outbursts occur usually in series separated by the orbital period. One explanation is that the companion star moves in a very eccentric orbit and accretes only matter when close to the compact object (Okazaki and Negueruela 2001). A large fraction of this subclass contain NS's. Also they are more concentrated towards the galactic center (Cornelisse et al. 2002). But this might be a consequence of observations mainly focusing on this region (Degenaar and Wijnands 2009).

Very Faint
Very Faint X-ray binaries have peak X-ray luminosity's of 10^{34-36} erg s^{-1}. There has been only one observation of a white dwarf system showing a outbursts above 10^{34} erg s^{-1} so VFXB's likely contains BH's and NS's (Watson et al. 1985). There have been several suggestions for explaining the very faint character. They could be intrinsically bright but appear as very faint due to their large distance (Wijnands et al. 2006). If these system are edge-on oriented the accretion disk can partly block X-rays (Muno et al. 2005). This way it appears as a very faint source but has a intrinsic luminosity that belongs to a bright source. Although it is more likely that these sources have a very faint intrinsic luminosity (Wijnands et al. 2006). As Wijnands et al. 2006 mentioned, different characteristics have been found in analysis of light curves and spectra from VFXB's and it seems to be a inhomogeneous

class with the distinction between faint and very faint rather arbitrary. Although we currently know that most sources in this class are low mass X-ray binaries.

3 The disc instability model

For Low mass X-ray binaries accretion happens via Roche lobe overflow. While material from the outer layers of the companion star is transferred towards the compact object angular momentum must be conserved and a accretion disk forms (Frank et al. 2002). Instabilities in this accretion disc can trigger the rise of outbursts. The disc instability model is the accepted description of outbursts in X-ray binaries (King and Ritter 1998). This model describes the effects of the disc irradiation on the disc stability. In NS binaries the irradiated accretion disk is caused by emission from the NS itself. In BH binaries it is the inner disc that irradiates the outer disc.

The disc instability model provides predictions for the outburst decay shape depending on the ionization state of the accretion disk. At the start of every outburst the accumulation of matter in the accretion disc is able to ionize the disc. The ionization raises the disc's viscosity which causes rapid rise in X-ray flux. When the accretion disk is fully ionized by irradiation from the central source a exponential decay is predicted. As soon as the outer edge of the disc cools down below the hydrogen ionization temperature the accretion disk becomes partly ionized. During this stage a linear decay is expected until it fades to quiescence. The transition from exponential to linear decay happens at a luminosity

$$L_t(NS) = 3.7 \times 10^{36} R_{11}^2 \text{erg s}^{-1} \tag{1}$$

for NS's and

$$L_t(BH) = 1.7 \times 10^{37} R_{11}^2 \text{erg s}^{-1} \tag{2}$$

for BH's. With R_{11} the accretion disc radius in units of 10^{11} cm and L_t the transition luminosity. Section 4.3 provides a explanation of how physical parameters were extracted from this model.

4 Method

From the about 30 known VFXB's we selected light curves that show a outburst and have enough data points to reveal a outburst shape. The selected X-ray light curves cover data from two telescopes: the Rossi X-ray Timing Explorer (*RXTE*) and the Neil Gehrels Swift Observatory (*Swift*). All the light curves from *RXTE* exlcuding *XTE J1118* which is taken with the All Sky Monitor (*ASM*), are taken with the the Proportional Counter Array (*PCA*) (ASM/RXTE; NASA; Swank and Markwardt 2001). The *PCA* and *ASM* have a energy range of 2–10keV .

Six *Swift* light curves are from the galactic center observing campaign (Degenaar et al. 2015). The other *Swift* light curves are processed via the online tool from (Evans et al. 2007). The X-ray telescope on board of *Swift* has two observing modes. Most of the time our sources are weak enough to be observed with the Photon Counting (*PC*) mode. But when the count rates reach the maximum of the *PC* mode *Swift* switches to Window Timing (*WT*) mode. In both modes the X-ray telescope on board *Swift* is sensitive to a energy range of 0.3-10keV. For the analysis on the *Swift* light curves we have used both observing modes.

4.1 Outburst duration τ_{dur}

Based on the symmetry of most outburst shapes, each outburst is fitted to a Gaussian using the `astropy` package (Astropy Collaboration and Robitaille 2013). From each Gaussian fit the standard deviation (*std*) is used to derive the duration of the outburst

$$\tau_{dur} = 6std \tag{3}$$

with τ_{dur} the outburst duration and *std* the standard deviation from the Gaussian fit. In order to get the best fit possible we have determined the average count rate and the standard deviation of the quiescence state:

1. **Fit-data selection**
   The standard deviation of the quiescence state is used as a tress hold for noise detection in the following way. For each outburst data points were selected from the top to earlier and later times until two adjacent observations have count rates below $2std$. This selected region is used as the input data for the Gaussian fit. For some *Swift* light curves containing solely the outburst region we used all data points.

2. **Offset count rates**.
   In order to get the best possible fit the light curve should as the Gaussian fit converge to zero in quiescence. Therefore all light curves count rates are subtracted by the average count rate of the quiescence. Light curves that show only the outburst region weren't corrected for the quiescence level.

For outbursts containing a few data points ($\sim$ 4) `astropy` can have trouble in finding the best fit and converge to amplitudes bigger then ten times the peak count rate. To avoid this behaviour the amplitude is constraint to

$$\text{amplitude} < 1.3 \times \text{peak rate} \tag{4}$$

4.2 Outburst decay time τ_{dec}

The second outburst parameter that is determined is the decay time τ_{dec}, also referred to the e-folding timescale computed over the outburst decay region (Chen et al. 1997). The decay time is, such as τ_{dur}, unrelated to instrumental sensitivity which makes it suitably for comparison between different sources from different telescopes. In order to extract τ_{dec} from each outburst a exponential function was fitted, using the `astropy` package. The exponential fit function is defined as

$$F(t) = A \exp\left(-\frac{t}{\tau_{dec}}\right) \tag{5}$$

with $F(t)$ the count rate, A the amplitude, t the time after the start of the outburst decay and τ_{dec} is the decay time. As mentioned earlier we fitted this decay model to the outburst decay region. This region is determined similarly as for τ_{dur} but the start point is fixed at the time of the peak rate. For some *Swift* light curves which are containing solely the decay region the whole data set was used.

The fit function 5 converges to zero moving forward in time. So the obtain the best fit the light curves should have a average count rate of zero when in quiescence. This correction is performed by subtracting the average of the background similar to τ_{dur}.

4.3 Decay model

At the beginning of the decay when the disc is completely ionized the outburst shows a exponential decay shape. At some time t_t the irradiation cannot maintain a fully ionized disc. When the disc becomes partially ionized the decay shape switch to linear. The exponential shape is described by

$$F(t) = (Ft - Fe)\exp\left(-\frac{t-t_t}{\tau_e}\right) + F_e \tag{6}$$

With $F(t)$ the count rate, F_t the count rate at the transition, F_e the exponential amplitude, t the time, τ_e the exponential decay time and t_t the time at the transition. The exponential amplitude is constraint to $0.4L_t \leqslant L_e \leqslant L_t$ based on Heinke et al. 2015. The linear shape is described by

$$F(t) = F_t\left(1 - \frac{t-t_t}{\tau_l}\right) \tag{7}$$

with $F(t)$ the count rate, F_t the count rate at the transition, t the time, t_t the time at the transition and τ_l the linear decay time. The final model thus looks like:

$$F(t) = \begin{cases} (6), & t \leqslant t_t. \\ (7), & t > t_t. \end{cases} \tag{8}$$

The model is fitted using Markov Chain Monte Carlo (*MCMC*) sampling. This is an improved version of the basic Monte Carlo sampling that produces a probability distribution from random start variables. The *MCMC* gives a probability distribution for each of the five parameters. The probability distribution lies between a chosen range and the meridian of the distribution is taken as the best fit value. Each parameter range is constraint by values matching with the outburst count rates.

Source selection
In order to fit this model to an outburst decay, the transition from a exponential to a linear decay must be clearly visible. In addition the number of data points at each side of the transition must be such that the difference between a totally exponential or linear decay is clear. For example some *Swift* light curves are having data points with intervals of one week which can't be used. But the *RXTE* light curves are have intervals of one day for which it is possible to distinct the exponential and linear part. The outbursts that meet these requirements are fitted with the decay model.

Accretion disk radius R_{circ}
With the fit parameters from this model several physical properties of the binary system can be derived. The first one is the radius of the accretion disk. This can be derived from

$$R_{disc} = 3.5 \times 10^7 \sqrt{\tau_e} \tag{9}$$

with R_{disc} the accretion disk radius and τ_e the exponential decay time (Heinke et al. 2015).

Orbital period P_{orb}
The second physical property that is determined is the orbital period P_{orb}. This orbital period is derived from the disc radius R_{disc} and the mass fraction q defined as the mass of the companion star divided by the mass of the compact object

$$P_{orb} = 3\left(\frac{R_{disc}}{R_\odot}\right)^{3/2}\frac{1}{(1+q)^2}\frac{1}{[0.500 - 0.227\log(q)]^6}\text{h} \tag{10}$$

with $R_\odot$ the mass of the Sun (Heinke et al. 2015).

Model validation
For sources with a known distance source d we are able to check if the model is corresponding to the theory with F_t. Therefore we converted count rates into flux with the Portable, Interactive Multi-Mission Simulator (*PIMMS*) tool (Mukai 1993). By replacing L_{acc} in equation 11 with the theoretical value from equations 1 or 2 and using the transition flux F_t from the fit we estimated the distance.

$$L_{acc} = 12\pi F d^2. \tag{11}$$

5 Results

5.1 Outburst detection

In total we found 41 outbursts in 21 sources listed in table 1. For each source we noted their confirmed compact object type, BH or a NS, in column 2. Sources with unknown compact object type are labeled with '?'. For each outburst the telescope used for observation and the time at the peak of the outburst is noted in column 2 and 3 respectively.

5 outbursts were classified as unsuitable to determine the duration or decay time via fitting:

- Two outbursts, *GR J17597-2201* and *IGR J1744-230*, contain outbursts with variable count rates longer than one year, they are classified as quasi periodic (QP) outbursts. The high variability of QP outbursts makes them unsuitable to determine the duration or decay time.
- The light curve of *IGR J17451-3022* also shows high variability in outburst so estimating the duration and decay time via fitting is not a realistic approximation.
- The *Swift* light curve of *SAX J1828.5-1037* shows a clear outburst at 55875MJD. But this outburst contains only data points at the top of the outburst which would result in big errors on the fit parameters.
- *XTE J1719-356* shows one clear increased count rate at 55376MJD in the *RXTE* light curve. The *Swift* light curve contains increased activity around the same time, shown in figure 1, which indicates that the increased activity in the *RXTE* light curve is real. Despite this increased activity, in the *RXTE* light curves there is now outburst shape visible besides this single data point. Additionally the *Swift* light curve does not show a clear outburst shape also duo to few data points. This makes it too hard to conclude anything about the duration or decay time of this outburst.

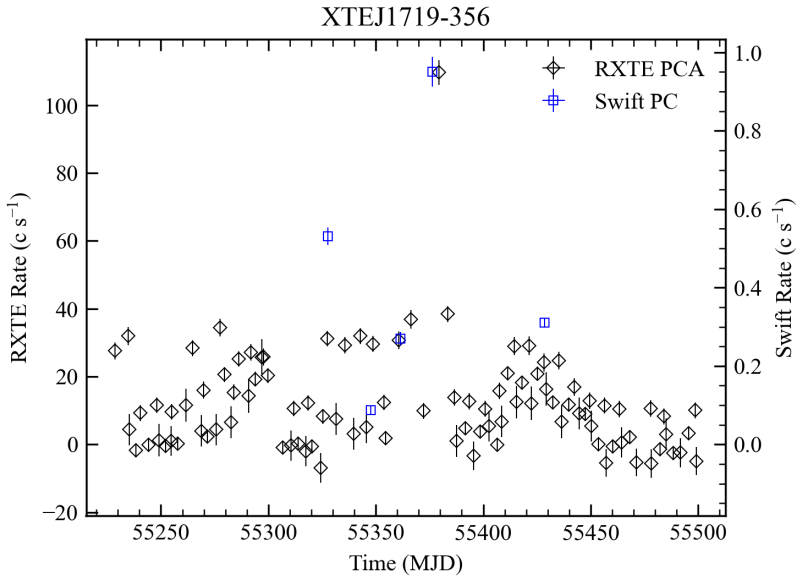

Fig. 1: The *RXTE* and *Swift* light curve of *XTE J1719-356* show increased activity around 55377MJD. This indicates that there is a outburst.

5.2 Duration

36 outbursts were successfully fitted to Gaussian function. The Gaussian fit of XTE J1728-295 is show in figure 2.

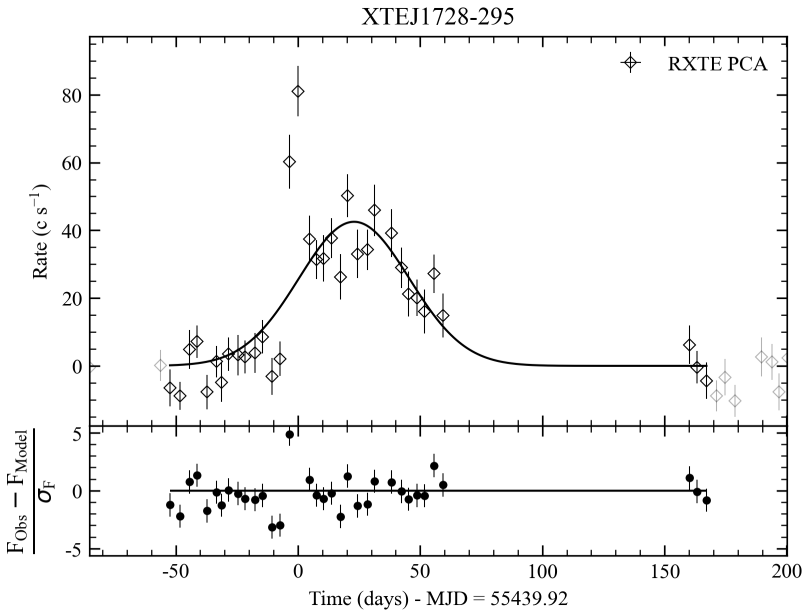

Fig. 2: Gaussian fit of a outburst from *XTE J1728-295*

Five outbursts (58584MJD *XTE J1728-295*, 56010MJD *IGR J1817-3656*, 55595MJD *Swift J1357.2-0933*, 57868MJD *Swift J1357.2-0933* and 54644MJD *XMMJ174457-2850.3*) weren't fit to a Gaussian because they only contain the decay part. The duration extracted from the fits is shown in column 5 of table 1. The distribution of the outburst's duration from all outbursts can be seen in figure 3.

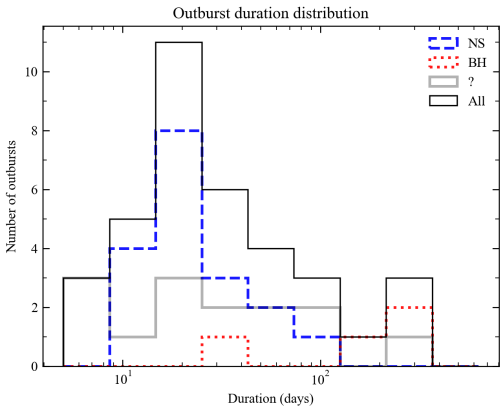

Fig. 3: Distribution of the outburst duration.

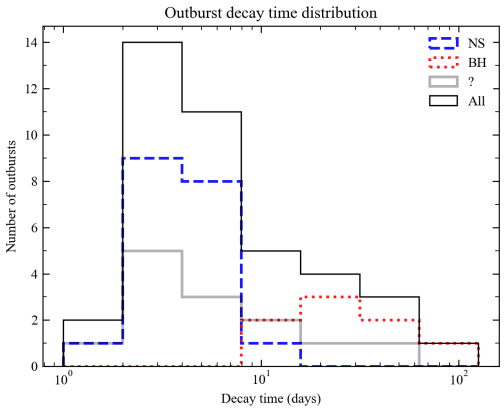

Fig. 4: Distribution of the outburst decay time.

5.3 Decay time

40 outbursts were successfully fitted to a exponential function. The Exponential fit of XTE J1728-295 is show in figure 5.

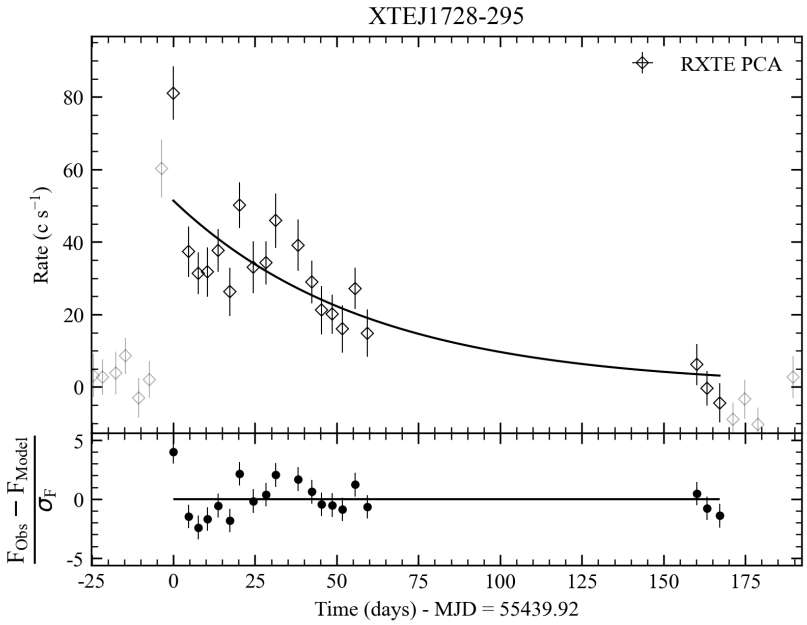

Fig. 5: Exponential fit of a outburst from *XTE J1728-295*

The outburst of *IGR J17375-3022* at 52466MJD has too few data points to resolve the outburst decay shape and produces a nonphysical decay time of 0.01. So this outburst decay time was excluded for analysis.

1 Source	2 BH/NS	3 Telescope	4 t_{peak} (MJD)	5 τ_{dur} r (days)	6 τ_{dec} (days)	7 Notes
XTE J1734-234	?	RXTE	51403	18.48	10.54	
IGR J17375-3022	?	RXTE	52466	5.940	0.01	
		RXTE	54750	7.380	2.41	
		RXTE	55043	7.440	1.89	
IGR J17597-2201	NS	RXTE	-	-	-	QP
		Swift	-	-	-	QP
SAX J1753.5-2349	NS	RXTE	51392	17.70	4.43	
		RXTE	54753	20.22	5.99	
		RXTE	55276	55.50	12.76	
WGA J1715.3-2635	?	RXTE	52501	113.72	26.86	
XTE J1118+480	BH	RXTE	51549	37.80	12.37	
	BH	RXTE	51693	321.51	76.31	
XTE J1637-498	?	RXTE	53215	17.70	2.73	
		RXTE	53818	29.90	3.28	
		RXTE	54707	30.20	5.67	
XTE J1719-291	NS	RXTE	54547	20.94	4.47	
XTE J1719-356	NS	RXTE	55376	-	-	U
		Swift	55379	-	-	U
XTE J1728-295	BH	RXTE	52927	261.45	22.21	
		RXTE	55440	135.62	59.77	
		Swift	58584	-	30.58	
XTE J1737-376	NS	RXTE	53053	15.33	3.05	
		RXTE	54714	21.09	7.09	
IGR J1744-230	?	RXTE	-	-	-	QP
IGR J1817-155	?	RXTE	54354	61.23	7.90	
IGR J1817-3656	BH	Swift	56010	-	11.26	
IGR J17451-3022	?	Swift	57056	-	-	HV
IGR J17494-3030	NS	Swift	56010	24.81	4.31	
SAX J1828.5-1037	?	Swift	55875	-	-	U
Swift J1357.2-0933	BH	Swift	55595	-	30.74	
		Swift	57868	-	35.86	
XMMJ174457-2850.3	NS	Swift	54644	-	2.53	
		Swift	55103	12.96	1.47	
		Swift	55408	10.09	2.24	
		Swift	56153	16.06	2.48	
		Swift	57659	13.89	2.77	
Swift J174553.7-290347	NS	Swift	53894	12.31	3.66	
Swift J174540.7-290015	?	Swift	57460	242.94	36.75	
Swift J174540.2-290037	?	Swift	57556	46.17	7.86	
		Swift		107.05	12.15	
Swift J174540.2-285921	?	Swift	55746	14.40	3.16	
		Swift	57578	16.61	2.93	
GRS 1741-2853	NS	Swift	54174	53.09	3.20	
		Swift	55112	40.76	5.02	
		Swift	55462	76.20	4.71	
		Swift	56517	33.19	2.21	
		Swift	57485	34.41	3.20	
		Swift	58045	24.39	7.77	

Tab. 1: All sources with their identified outbursts. For each source the type of compact object BH, NS or unkown ? is specified. For each outburst we noted from which telescope the observation data originates, the time at the peak of the outburst, the outburst duration, the outburst decay time and possible notifications. Notes dictionary; QP: Quasi Periodic outburst, U: Unclear outburst shape due to few data points which make it unsuitable for fitting and HV: High Variability in outburst making it not suitable for fitting.

5.4 Decay model

1 Source	2 F_t ($c\ s^{-1}$)	3 F_e ($c\ s^{-1}$)	4 τ_e (days)	5 τ_l (days)	6 t_t (MJD)
SAX J1753.5-2349	32.434±0.046	30.479±0.054	5.999±0.562	7.954±0.572	55298.3±1.1
XTE J1118+480	2.291*	2.133±0.01	3.382±0.707	18.452±1.346	51556.3±0.8
XTE J1118+480	2.291±0.01	2.275±0.01	15.801±6.357	30.735±4.681	51727.0±3.1
XTE J1737-376	20.845±0.034	10.093±0.080	6.124±0.331	1.935 ±0.530	54728.4±0.5
XTE J1728-295	4.571 10^{-11} ± 0.012	2.009 10^{-11} ± 0.033	20.216±0.685	92.049 ±1.850	58629.3±1.4
IGR J17177-3656	1.652 10^{-1} ± 0.041	6.855 10^{-2} ± 0.045	10.863±0.250	15.877±1.376	55662.1±1.4
XMM J174457-2850.3	3.273 10^{-2} ± 0.115	1.706 10^{-2} ± 0.155	2.242±0.238	3.975±0.831	54651.3±0.8

SAX J1753.5-2349

Equation 9 gives a disk radius of 2.520 10^{10} cm. This source is known as a NS binary so we assumed that $q = 0.1$. This disc radius together with the mass ratio gives a orbital period of 3.656±0,342h via equation 10.

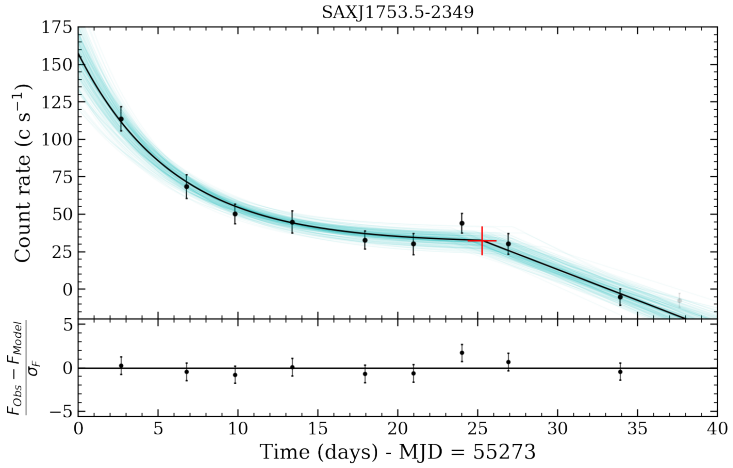

Fig. 6: Decay model fit of *SAX J1753.5-2349*

XTE J1118+480

There are two outbursts from *XTE J1118+480* visible in its light curve. The fit of the outburst at 51693 MJD gives a disk radius of 4.089 10^{10} cm by equation 9. This disc radius together with a mass fraction 0.037±0.007 give a orbital period of 3.4h±0.7 via equation 10. Analysis on the outburst at 53215 MJD can be found in the discussion. Based on the transition flux F_t this source should be at a distance of 3.074±0.037 kpc with $n_h = 0.99\ 10^{22}$ based on Stoop et al. 2021.

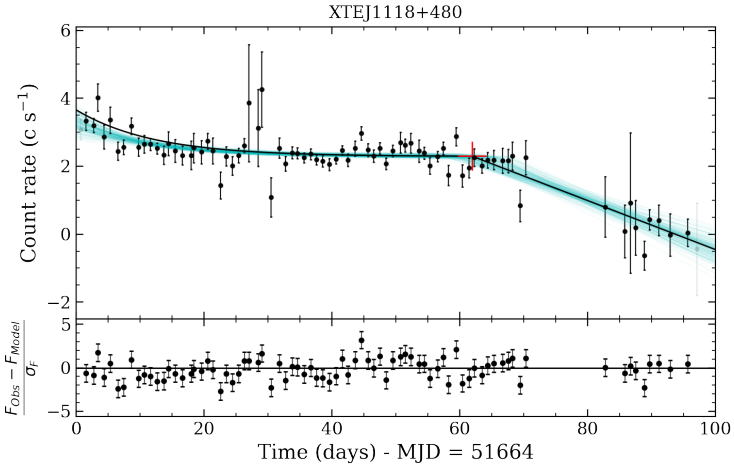

Fig. 7: Decay model fit of *XTE J1118+480*

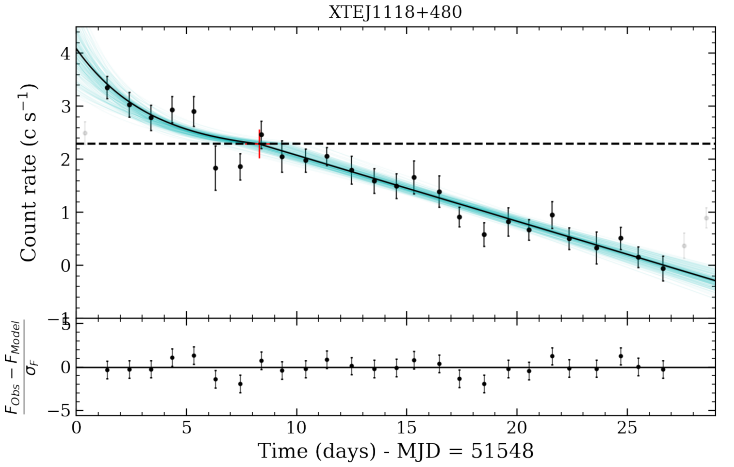

Fig. 8: Decay model fit of *XTE J1118+480*

XTE J1737-376

Equation 9 gives a disk radius of 2.546 10^{10} cm. This disc radius together with a mass ratio of $q = 0.04$ (Sanna et al. 2018) gives a orbital period of 2.05$\pm$0.10h via equation 10.

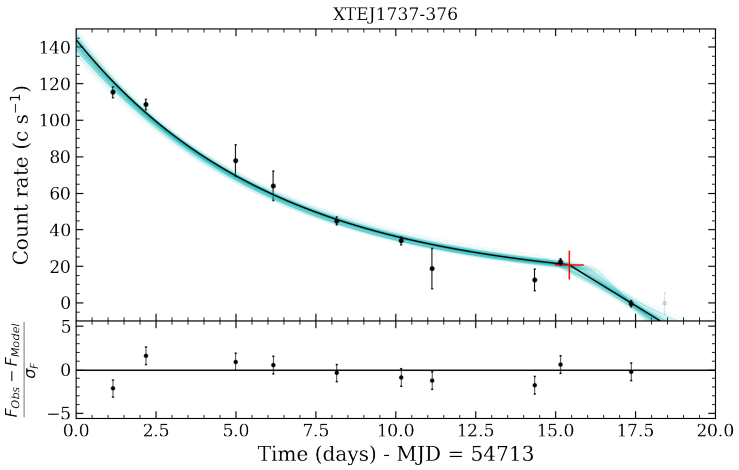

Fig. 9: Decay model fit of *XTE J1737-376*

XTE J1728-295

Assuming $q = 0.01$ gives a orbital period of 2.17±0.05h via equation 10 as in Stoop et al. 2021.

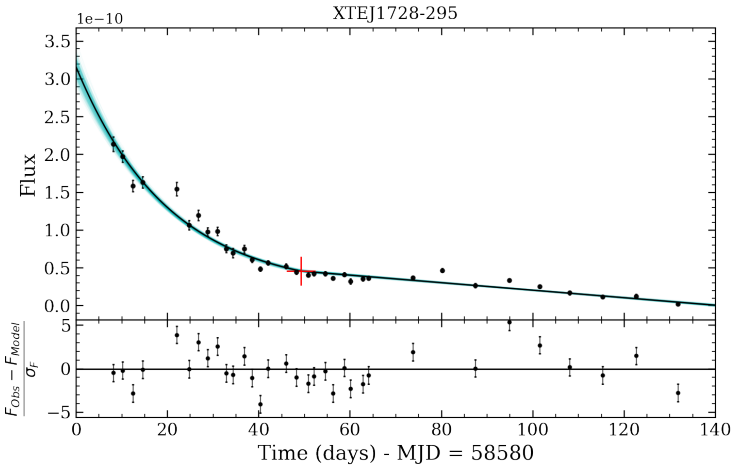

Fig. 10: Decay model fit of *XTE J1728-295*

IGR J17177-3656

Equation 9 gives a disk radius of 3.390 10^{10} cm. This disc radius together with a mass ratio of $q = 0.1$ gives a orbital period of 5.70±0.13h via equation 10.

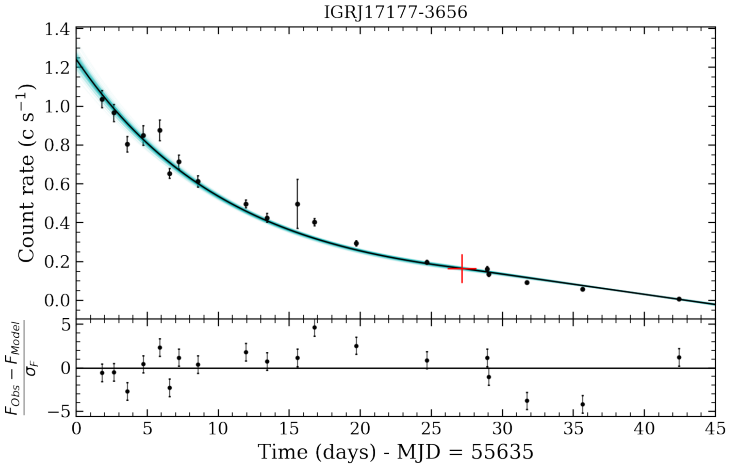

Fig. 11: Decay model fit of *IGR J17177-3656*

XMMJ174457-2850.3

Assuming $q = 0.01$ gives a orbital period of 1.81 ± 0.12h via equation 10 as in Heinke et al. 2015.

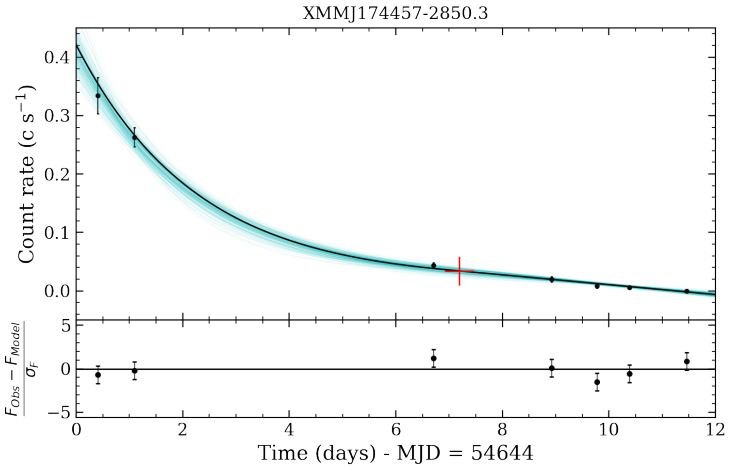

Fig. 12: Decay model fit of *XMMJ174457-2850.3*

6 Discussion

6.1 Typical duration and decay time

The duration and decay time distribution shows a similar trend to that of brighter sources (Yan and Yu 2015). This gives indications for a similar accretion process in both bright and very faint sources. Still it are indications since it is low number statistics. Secondly we noticed that BH's seems to have longer outbursts and decay times. Most BH's we observe are having a large accretion discs and therefore longer outbursts and decay times which explains the difference between NS's and BH's in the distributions Wu et al. 2010.

It has to be mentioned that **?** used other methods to determine the duration and decay time. We have tested their method on *WGAJ1715.3-2635* and found a duration more than 6 times larger than the selected outburst region. In their method they are selecting data points above a certain percentage from the peak rate. Because most light curves from VFXB's have low count rates and therefore higher noise levels this methods turned out to be useful.

6.2 Orbital periods

For all 6 sources we have found orbital periods of 1.81h to 5.70h which matches with the expectation from Wu et al. 2010. For *XTEJ1118+480* we obtained a distance of 3.074 ± 0.037 kpc which is matching with observations ranging from 3 to 8 kpc (Gandhi et al. 2019). Also we checked the transition luminosity by fitting the first outburst to the decay model while fixing F_t to the value of the second outburst. This fit is shown in figure 8 and it seems a reasonable fit indicating the transition luminosity is the same in both outbursts. For *XTE J1737-376* the orbital period was found to be 2.05 ± 0.10h which matches witch $\sim$1.9h from Sanna et al. 2018. This gives indications that the disc instability model can be used for VFXB's that show a clear transition.

Most outbursts do not contain enough data points which makes the identification of a transition from exponential to linear decay difficult. Also in most light curves of VFXB's count rates are low and therefore hard to conclude if the model is working better than a complete linear or exponential for example. But for 7 outbursts the results look promising combined with the fact that observations match on 2 sources giving strong indications the decay model works. Therefore it is interesting to use and test the validity of this model further on future outbursts.

7 Conclusion

We have performed a first systematic study of outburst light curves from 21 VFXB's. Similar trend as in bright X-ray binaries in the distribution for the duration and decay time have been found indicating a similar accretion process. Black holes seem to have longer outbursts and decay times explained by the larger accretion disks of BH's. Using the disc instability model we have found orbital periods of 2 to 5 hours witch as expected also indicating no different accretion process. For two sources the disc instability model predicts a orbital period and distance matching with observations. So far data quality is the most limitating factor to fit the disc instability model but more outburst showing enough data points to identify a transition are needed to test the instability model at a more convincingly way.

References

ASM/RXTE. RXTE ASM lightcurves. URL http://xte.mit.edu/asmlc/ASM.html.

Astropy Collaboration and Thomas P. Robitaille. Astropy: A community Python package for astronomy. , 558:A33, October 2013. doi: 10.1051/0004-6361/201322068.

Wan Chen, C. R. Shrader, and Mario Livio. The Properties of X-Ray and Optical Light Curves of X-Ray Novae. , 491(1):312–338, December 1997. doi: 10.1086/304921.

R. Cornelisse, F. Verbunt, J. J. M. in't Zand, E. Kuulkers, J. Heise, R. A. Remillard, M. Cocchi, L. Natalucci, A. Bazzano, and P. Ubertini. BeppoSAX Wide Field Cameras observations of six type I X-ray bursters. , 392:885–893, September 2002. doi: 10.1051/0004-6361:20020707.

N. Degenaar and R. Wijnands. The behavior of subluminous X-ray transients near the Galactic center as observed using the X-ray telescope aboard Swift. , 495(2):547–559, February 2009. doi: 10.1051/0004-6361:200810654.

N. Degenaar, R. Wijnands, J. M. Miller, M. T. Reynolds, J. Kennea, and N. Gehrels. The Swift X-ray monitoring campaign of the center of the Milky Way. *Journal of High Energy Astrophysics*, 7: 137–147, September 2015. doi: 10.1016/j.jheap.2015.03.005.

P. A. Evans, A. P. Beardmore, K. L. Page, L. G. Tyler, J. P. Osborne, M. R. Goad, P. T. O'Brien, L. Vetere, J. Racusin, D. Morris, D. N. Burrows, M. Capalbi, M. Perri, N. Gehrels, and P. Romano. An online repository of Swift/XRT light curves of γ-ray bursts. , 469(1):379–385, July 2007. doi: 10.1051/0004-6361:20077530.

Juhan Frank, Andrew King, and Derek J. Raine. *Accretion Power in Astrophysics: Third Edition*. 2002.

Poshak Gandhi, Anjali Rao, Michael A. C. Johnson, John A. Paice, and Thomas J. Maccarone. Gaia Data Release 2 distances and peculiar velocities for Galactic black hole transients. , 485(2):2642–2655, May 2019. doi: 10.1093/mnras/stz438.

C. O. Heinke, A. Bahramian, N. Degenaar, and R. Wijnands. The nature of very faint X-ray binaries: hints from light curves. *Monthly Notices of the Royal Astronomical Society*, 447(4):3034–3043, 01 2015. ISSN 0035-8711. doi: 10.1093/mnras/stu2652. URL https://doi.org/10.1093/mnras/stu2652.

A.R. King and H. Ritter. The light curves of soft X-ray transients. *Monthly Notices of the Royal Astronomical Society*, 293(1):L42–L48, 01 1998. ISSN 0035-8711. doi: 10.1046/j.1365-8711.1998.01295.x. URL https://doi.org/10.1046/j.1365-8711.1998.01295.x.

Jean-Pierre Lasota. The disc instability model of dwarf novae and low-mass X-ray binary transients. , 45(7):449–508, June 2001. doi: 10.1016/S1387-6473(01)00112-9.

Q. Z. Liu, J. van Paradijs, and E. P. J. van den Heuvel. A catalogue of low-mass X-ray binaries in the Galaxy, LMC, and SMC (Fourth edition). , 469(2):807–810, July 2007. doi: 10.1051/0004-6361:20077303.

K. Mukai. PIMMS tool. *Legacy*, 3:21–31, October 1993.

M. P. Muno, J. R. Lu, F. K. Baganoff, W. N. Brandt, G. P. Garmire, A. M. Ghez, S. D. Hornstein, and M. R. Morris. A remarkable low-mass x-ray binary within 0.1 parsecs of the galactic center. *The Astrophysical Journal*, 633(1):228–239, nov 2005. doi: 10.1086/444586. URL https://doi.org/10.1086/444586.

NASA. RXTE Galactic Center PCA lightcurves. URL https://asd.gsfc.nasa.gov/Craig.Markwardt//galscan/main.html.

Mason Ng, Paul S. Ray, Peter Bult, Deepto Chakrabarty, Gaurava K. Jaisawal, Christian Malacaria, Diego Altamirano, Zaven Arzoumanian, Keith C. Gendreau, Tolga Güver, Matthew Kerr, Tod E. Strohmayer, Zorawar Wadiasingh, and Michael T. Wolff. NICER Discovery of Millisecond X-Ray Pulsations and an Ultracompact Orbit in IGR J17494-3030. , 908(1):L15, February 2021. doi: 10.3847/2041-8213/abe1b4.

A. T. Okazaki and I. Negueruela. A natural explanation for periodic X-ray outbursts in Be/X-ray binaries. , 377:161–174, October 2001. doi: 10.1051/0004-6361:20011083.

Craig R. Powell, Carole A. Haswell, and Maurizio Falanga. Mass transfer during low-mass X-ray transient decays. , 374(2):466–476, January 2007. doi: 10.1111/j.1365-2966.2006.11144.x.

A. Sanna, E. Bozzo, A. Papitto, A. Riggio, C. Ferrigno, T. Di Salvo, R. Iaria, S. M. Mazzola, N. D'Amico, and L. Burderi. Xmm-newton detection of the 2.1 ms coherent pulsations from igr j17379–3747. *Astronomy Astrophysics*, 616:L17, Aug 2018. ISSN 1432-0746. doi: 10.1051/0004-6361/201833205. URL http://dx.doi.org/10.1051/0004-6361/201833205.

Jean Swank and Craig Markwardt. Populations of Transient Galactic Bulge X-ray Sources. 251:94, January 2001.

M. A. P. Torres, P. J. Callanan, M. R. Garcia, P. Zhao, S. Laycock, and A. K. H. Kong. MMT observations of the black hole candidate XTE j1118480 near and in quiescence. *The Astrophysical Journal*, 612(2):1026–1033, sep 2004. doi: 10.1086/422740. URL https://doi.org/10.1086/422740.

M. G. Watson, A. R. King, and J. Osborne. The old nova GK Per : discovery of the X-ray pulse period. , 212:917–930, February 1985. doi: 10.1093/mnras/212.4.917.

R. Wijnands, J. J. M. in 't Zand, M. Rupen, T. Maccarone, J. Homan, R. Cornelisse, R. Fender, J. Grindlay, M. van der Klis, E. Kuulkers, and et al. Thexmm-newton/chandramonitoring campaign of the galactic center region. *Astronomy Astrophysics*, 449(3):1117–1127, Mar 2006. ISSN 1432-0746. doi: 10.1051/0004-6361:20054129. URL http://dx.doi.org/10.1051/0004-6361:20054129.

Y. X. Wu, W. Yu, T. P. Li, T. J. Maccarone, and X. D. Li. Orbital Period and Outburst Luminosity of Transient Low Mass X-ray Binaries. , 718(2):620–631, August 2010. doi: 10.1088/0004-637X/718/2/620.

Zhen Yan and Wenfei Yu. X-Ray Outbursts of Low-mass X-Ray Binary Transients Observed in the RXTE Era. , 805(2):87, June 2015. doi: 10.1088/0004-637X/805/2/87.

8 Apendix

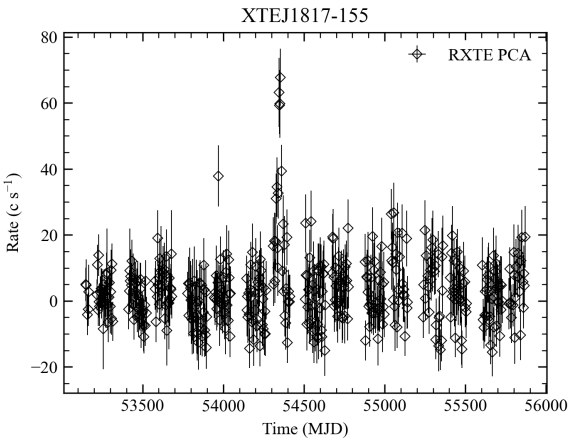
XTEJ1817-155
RXTE PCA
Rate (c s^{-1})
Time (MJD)

(a)

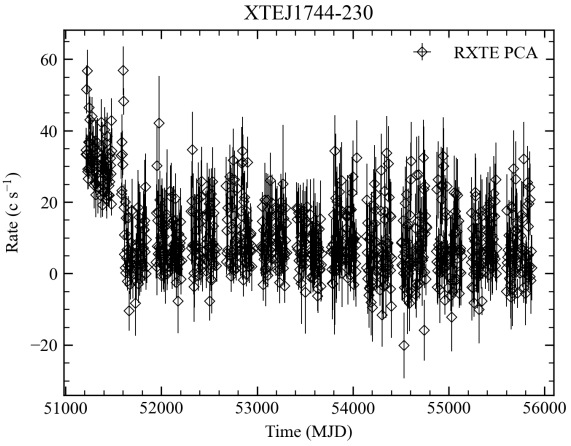
XTEJ1744-230
RXTE PCA
Rate (c s^{-1})
Time (MJD)

(b)

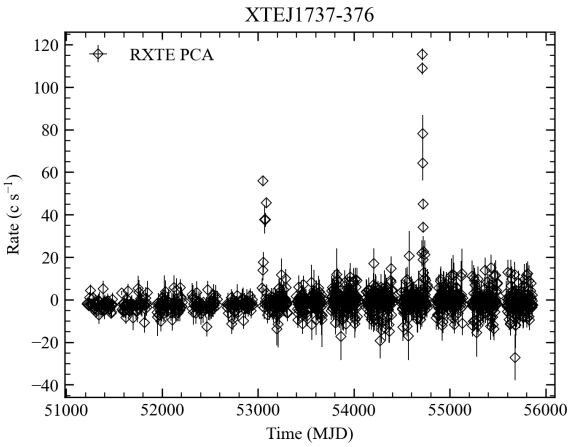
XTEJ1737-376
RXTE PCA
Rate (c s^{-1})
Time (MJD)

(c)

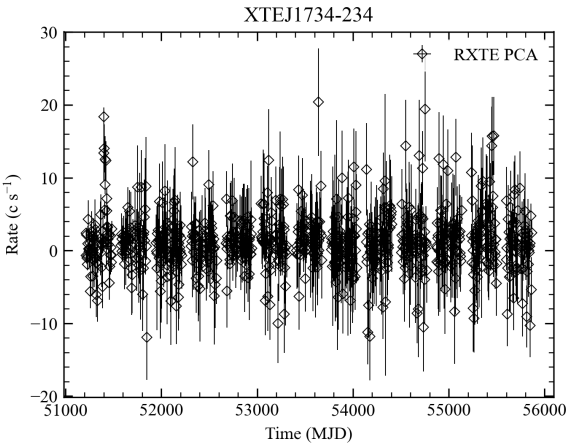
XTEJ1734-234
RXTE PCA
Rate (c s^{-1})
Time (MJD)

(d)

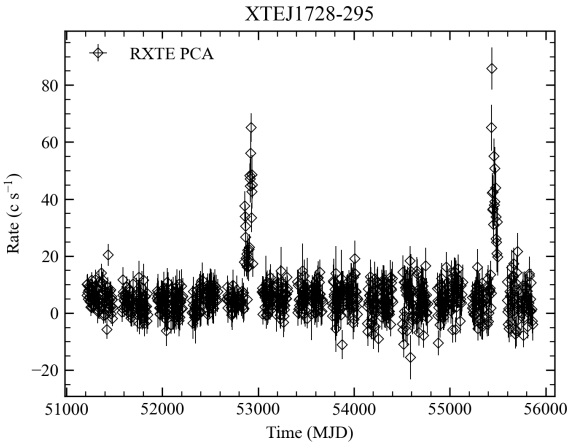
XTEJ1728-295
RXTE PCA
Rate (c s^{-1})
Time (MJD)

(e)

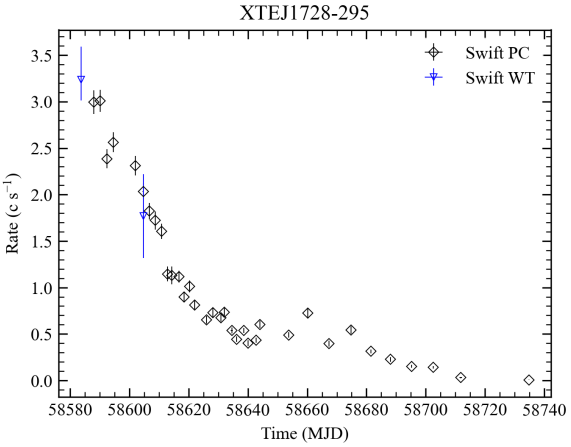
XTEJ1728-295
Swift PC
Swift WT
Rate (c s^{-1})
Time (MJD)

(f)

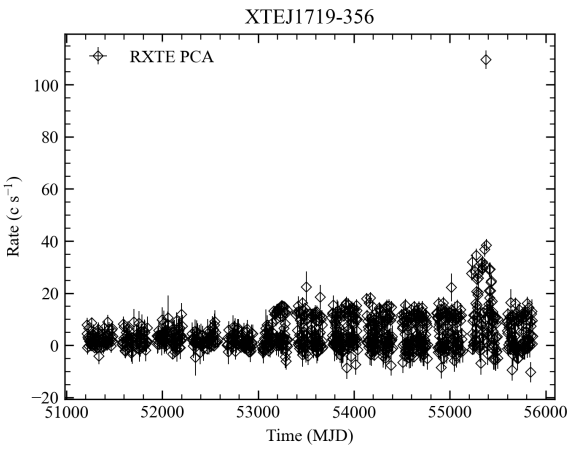
XTEJ1719-356
RXTE PCA
Rate (c s^{-1})
Time (MJD)

(g)

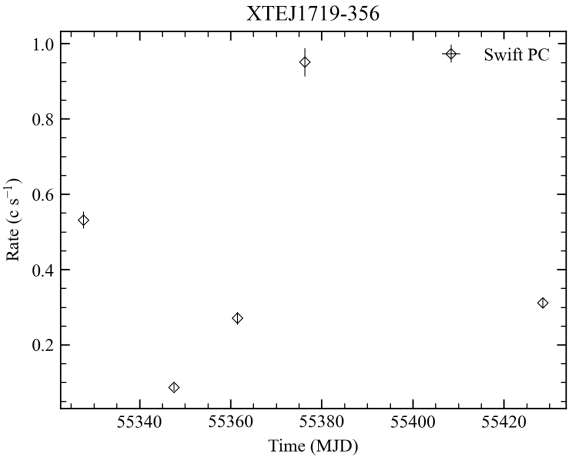
XTEJ1719-356
Swift PC
Rate (c s^{-1})
Time (MJD)

(h)

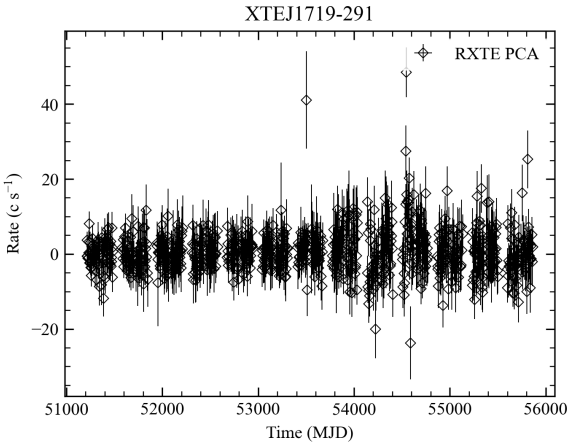
XTEJ1719-291
RXTE PCA
Rate (c s^{-1})
Time (MJD)

(i)

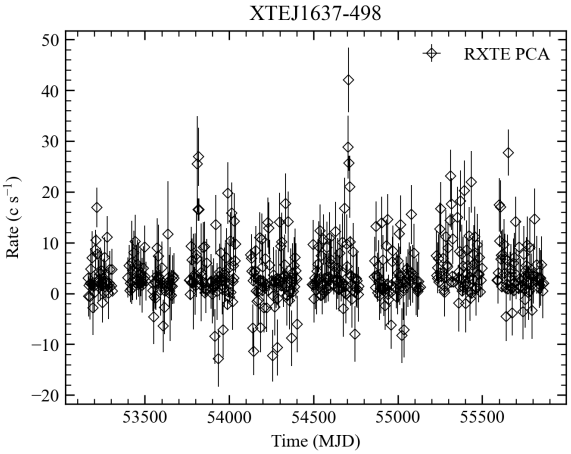
XTEJ1637-498
RXTE PCA
Rate (c s^{-1})
Time (MJD)

(j)

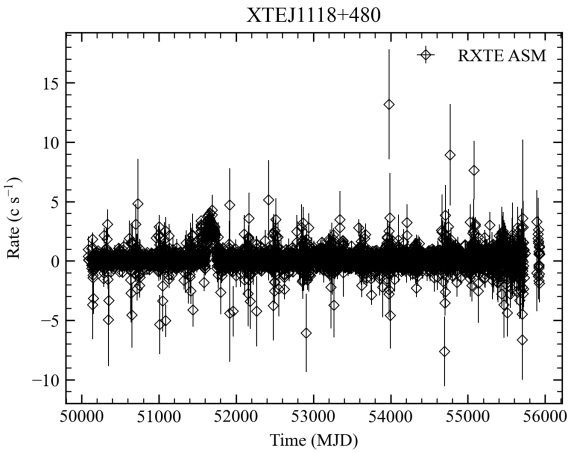
XTEJ1118+480
RXTE ASM
Rate (c s^{-1})
Time (MJD)

(k)

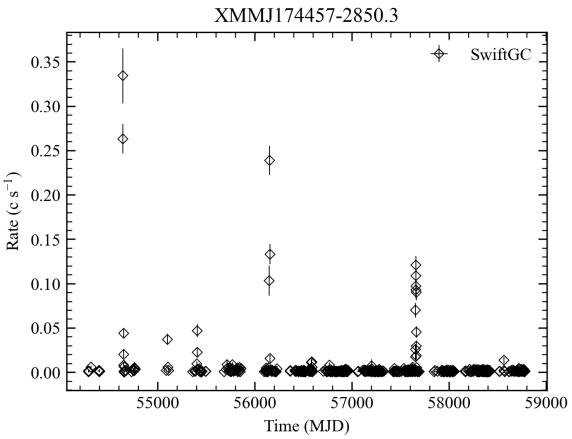
XMMJ174457-2850.3
SwiftGC
Rate (c s^{-1})
Time (MJD)

(l)

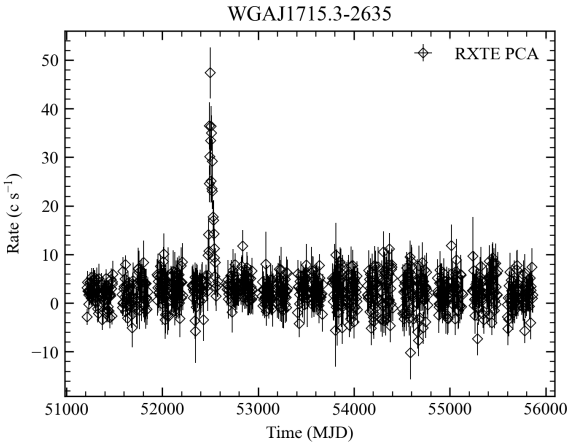
WGAJ1715.3-2635
RXTE PCA
Rate (c s^{-1})
Time (MJD)

(m)

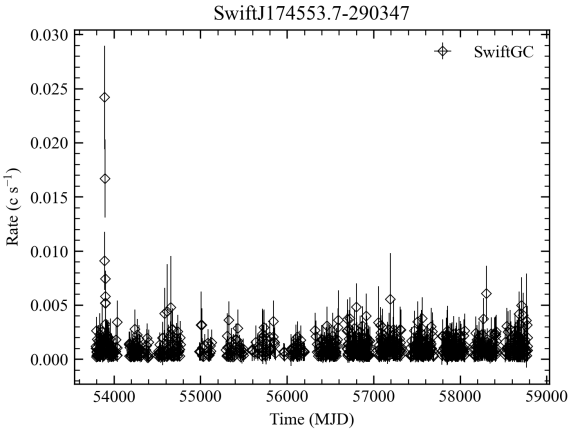
SwiftJ174553.7-290347
SwiftGC
Rate (c s^{-1})
Time (MJD)

(n)

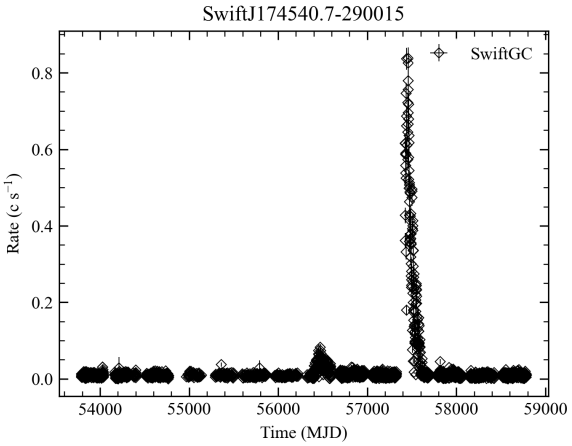
SwiftJ174540.7-290015
SwiftGC
Rate (c s^{-1})
Time (MJD)

(o)

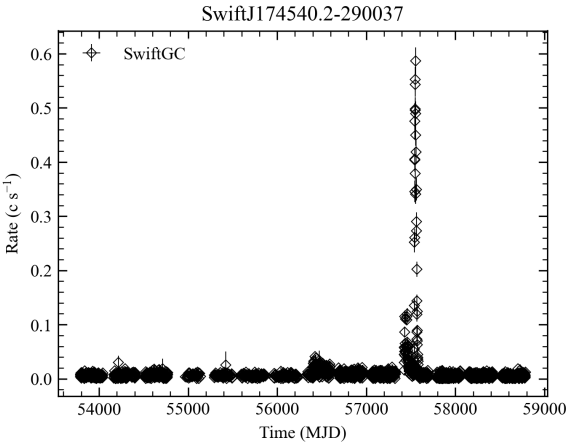
SwiftJ174540.2-290037
SwiftGC
Rate (c s^{-1})
Time (MJD)

(p)

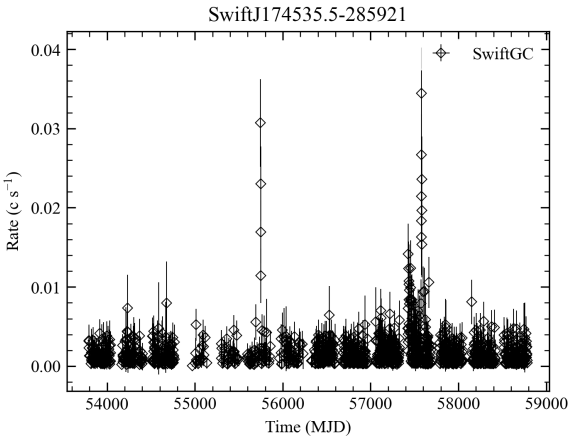
SwiftJ174535.5-285921
SwiftGC
Rate (c s^{-1})
Time (MJD)

(q)

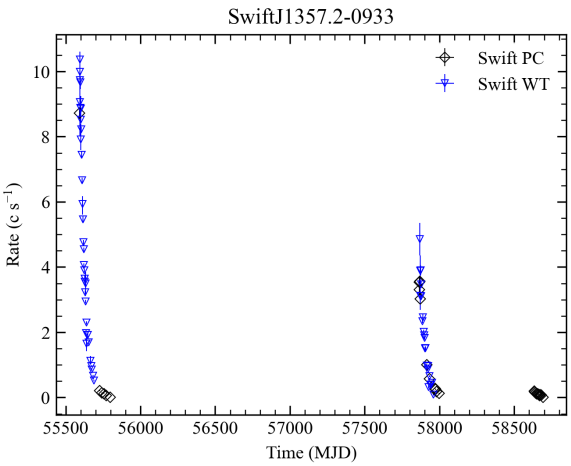
SwiftJ1357.2-0933
Swift PC
Swift WT
Rate (c s^{-1})
Time (MJD)

(r)

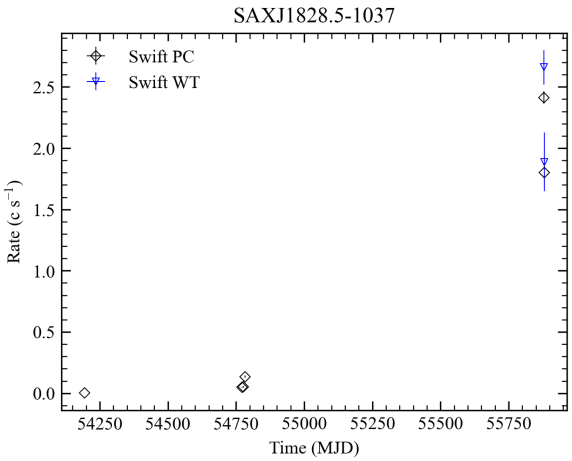
SAXJ1828.5-1037
Swift PC
Swift WT
Rate (c s^{-1})
Time (MJD)

(s)

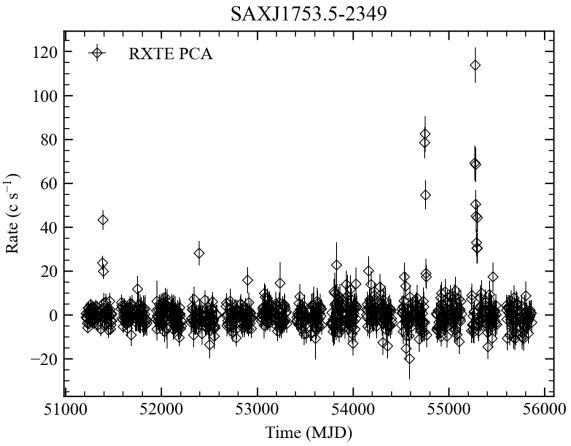
SAXJ1753.5-2349
RXTE PCA
Rate (c s^{-1})
Time (MJD)

(t)

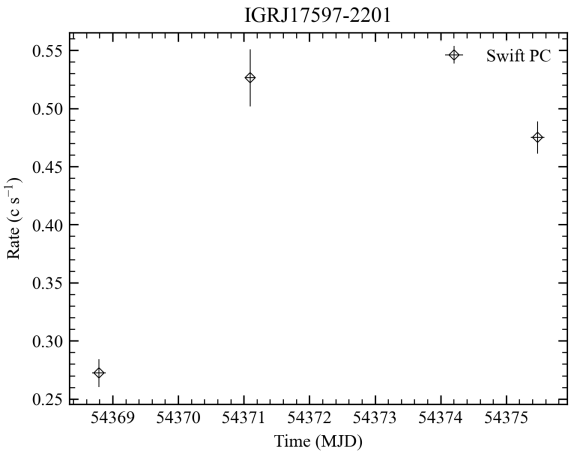
IGRJ17597-2201
Swift PC
Rate (c s^{-1})
Time (MJD)

(u)

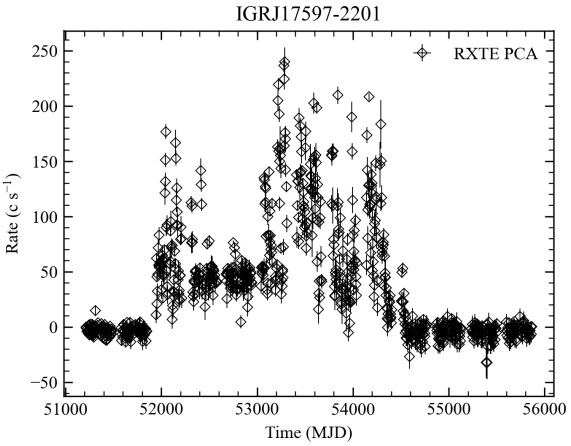
IGRJ17597-2201
RXTE PCA
Rate (c s^{-1})
Time (MJD)

(v)

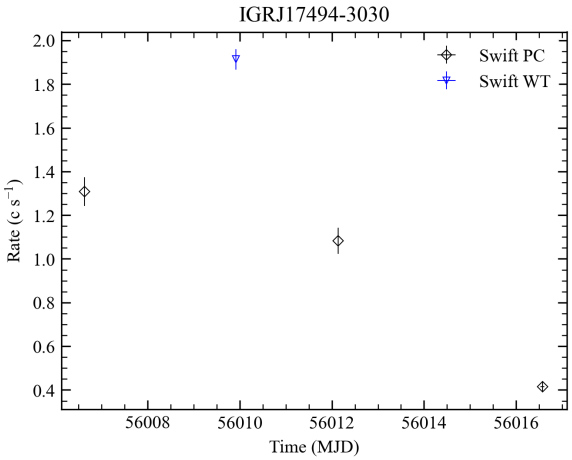
IGRJ17494-3030
Swift PC
Swift WT
Rate (c s^{-1})
Time (MJD)

(w)

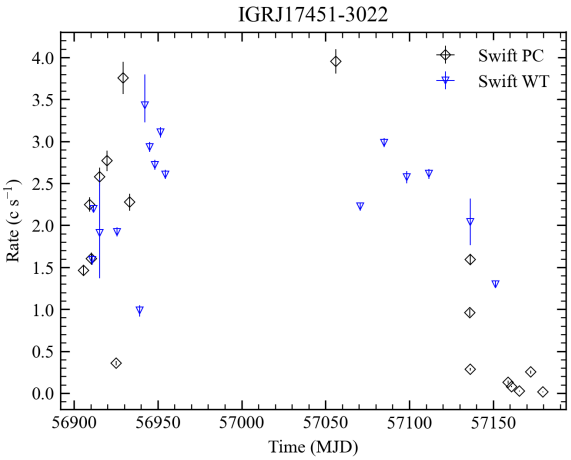
IGRJ17451-3022
Swift PC
Swift WT
Rate (c s^{-1})
Time (MJD)

(x)

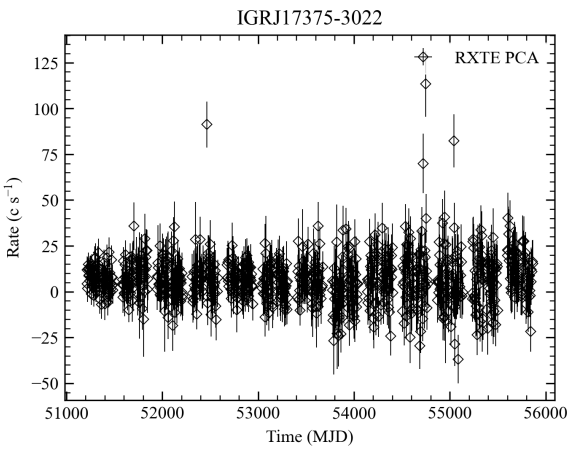
IGRJ17375-3022
RXTE PCA
Rate (c s^{-1})
Time (MJD)

(y)

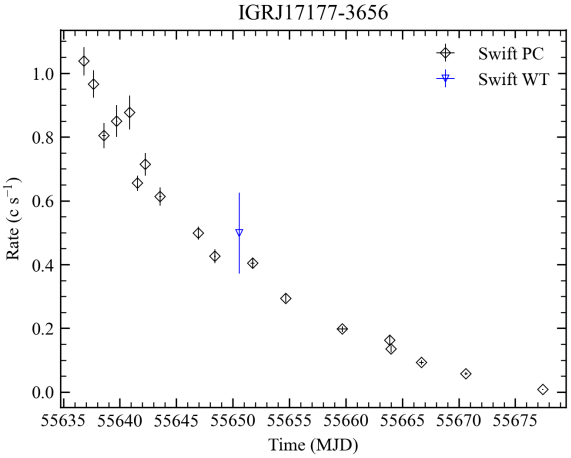
IGRJ17177-3656
Swift PC
Swift WT
Rate (c s^{-1})
Time (MJD)

(z)

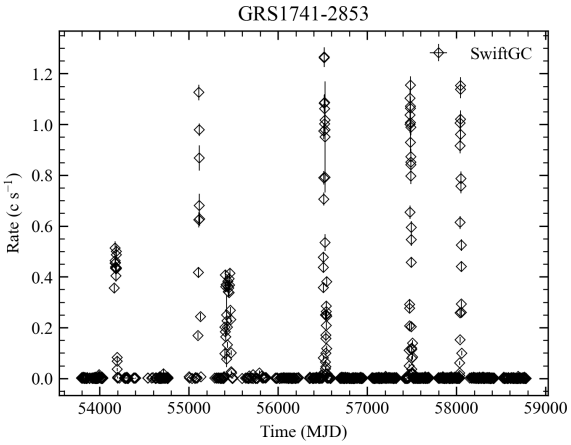
GRS1741-2853
SwiftGC
Rate (c s^{-1})
Time (MJD)

()